IUG Journal of Natural Studies
Peer-reviewed Journal of Islamic University-Gaza

ISSN 2790-1653

IUGNS
Vol 32, No 01, 2024, pp 06-13

Curie temperature points and AC electric properties of Li-ferrite replaced by divalent Ni^{2+} ions

Samy K.K. Shaat [1,*]
Elham A. Elhillo [1]
Hussain A. Dawoud[1]

[1]Department of Physics, Faculty of Science, Islamic University of Gaza, Gaza Strip, Palestine

*** Corresponding author**
e-mail address: samyshaat@yahoo.com

https://doi.org/10.33976/IUGNS.32.1/2024/2

Abstract:
In the present work, Curie temperature points, electric and dielectric properties were investigated for $Ni_xLi_{0.5(1-x)}Fe_{2.5-0.5x}O_4$ spinel ferrite, which were prepared using the standard ceramic technique. Curie temperature points decreasing with increasing of the Ni^{2+} ions. With increasing frequency of the external source, permittivity constant and loss tangent reduced continuously, while AC conductivity increased. This variation of electric properties was elucidated based on $Fe^{3+} + e^- = Fe^{2+}$ and $Ni^{2+} + h^+ = Ni^{3+}$.

Keywords:
Spinel
Ferrite
Electric Properties
Dielectric Properties
Induction
Curie temperature

1. Introduction:

Due to their low conductivity, low loss tangent, and low cost, lithium ferrites and their additions are regarded as one of the crucial materials for a wide range of applications (Dawoud et al 2018, Aravind et al 2014). Spinel Li-ferrites have a wide range of fascinating features due to their capacity to incorporate a variety of transition metal cations into their crystal, resulting in changes in optical, structural, mechanical and electromagnetic properties. This is because the degree of inversion in substituted lithium ferrites and, consequently, their properties, are found to be highly dependent on the production parameters (method of preparation, sintering duration, sintering temperature, etc.), amount of substituent, and type of substitution (Aravind et al 2014). Substituted Li-ferrites have emerged as one of the most appealing materials for microwave applications, particularly as a garnet substitute. Mixed Li-ferrites are attractive materials for microwave applications due to their inexpensive cost, square hysteresis loop, and high Curie temperature. Many studies have examined the inclusion of 2+, 3+, and 4+ ions in Li-ferrites (Khot Sujata et al 2014) such as Li-Zn (Dawoud et al 2018) and Li-Cu (Mazen et al 1999) in addition to pure Li-ferrites. Herein, this work focuses on Ni-Li spinel ferrite. This current work aims to determine Curie temperature points, in addition, to investigate the

influence of adding Ni^{2+} ions to Li-spinel ferrite on AC electric conductivity and dielectric parameters, with the detailed investigation of the composition.

2. Methods

$Ni_xLi_{0.5(1-x)}Fe_{2.5-0.5x}O_4$ where $0.0 \leq x \leq 1.0$ with step 0.2 were synthesised via traditional technique more detail are found elsewhere [Dawoud et al 2018]. In the beginning, high purity Li_2CO_3, NiO and Fe_2O_3 were milled manually to a fine powder for 5 hours according to x percentage for each sample using mortar and pestle. After that, the milled powder were presintered at 750 ℃ soaking time of 3 hours, followed by, re-grinding manually for 3 hours using mortar and pestle, then ecah one was compresseded at $3 \times 10^8\ pa$ in circular shape (with a radius $R = (3.8 - 9.1\ mm)$ and width $w = 3 - 5\ mm$ and toroidal shape (outer and inner radius are $r_o = 8.24\ mm$ and $r_i = 3.98\ mm$, respectively, with thickness ($w = 3 - 5\ mm$). Finally, samples were sintered at 1000 ℃ for soaking time of 20 hours. After sintering, the samples were left to cool slowly to room temperature. Following cooling, the circular samples were polished to create round discs with two uniform parallel surfaces, which may be used for determining the dielectric constant, dielectric loss tangent, and AC electric conductivity (σ_{AC}), The toroidal samples were polished to obtain a uniform shape to be suitable to determine Curie temperature points (T_C). The following Eqn. using to calculate initial permeability (μ_i)

$$\mu_i = \frac{2\pi L}{\mu_o N^2 w \ln(r_o/r_i)} \quad (1)$$

where N is the number of turns, μ_o is the permeability of the free sample, and L is the inductance. According to Scheme 1, L was determined with an accuracy of (0.05%) using an LCR meter model (GW- instek LCR-821) with a series circuit, an applied voltage of 1 V, and a constant frequency of 20 kHz. At room temperature, the dielectric constant, the σ_{AC}, and the dielectric loss tangent were measured using the double probe electrode method.

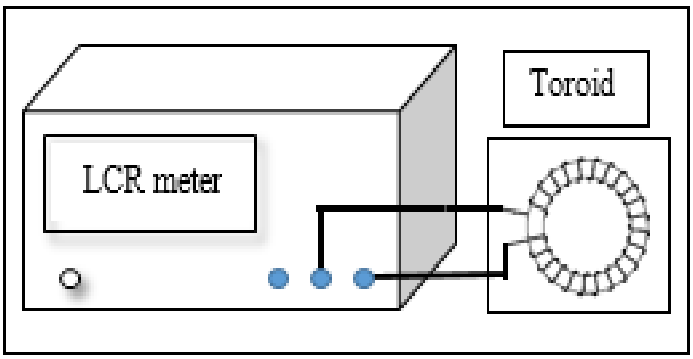

Scheme 1 ***A diagram for measuring the inductance of the toroidal samples of the mixed Li-Ni spinel ferrite.***

Variation of μ_i versus temperature for all samples are given in Fig. 1. As can be seen in this Figure, μ_i grows as the temperature increases until it reaches TC, then it drops sharply. This means that the state of the sample changes from ferrimagnetic to paramagnetic state. In addition, it can be noted from Fig. 1, that the value of TC decreasing with increasing of Ni^{2+} ions. This behavior agrees well with the results in refs. (Dawoud et al 2016, Aravind et al 2915). The decreasing in TC can be explained according to suggested cations distribution $(Fe^{3+}_{(1)})_T\{Li^{1+}_{0.5(1-x)}Ni^{2+}_xFe^{3+}_{1.5-0.5x}\}_OO^{2+}_4$ [1]. According to Table 1, the cation distribution depends on the spin (low and high) diagrams of crystal field splitting of cation 3d orbitals in the case of tetrahedral (( )$_T$) as well as octahedral ({}$_O$) symmetries in spinel-type Li-Ni ferrite. Therefore, the different distribution of cation means that the spin-orbit interaction, the band gap, …,etc, will be

varied. This implies to have different properties for the given materials and so, different applications. Consequently, when adding Ni^{2+} ions to Li-ferrite, they will reduce Li^{+} ions at Oh sites i.e., the number of Fe^{3+} ions will reduce at Oh sublattices. Regardless of the number of links or linkages between magnetic ions, this tends to strengthen Td and Oh exchange interactions of the kind ($Fe_T^{3+} - O^{2-} - Fe_O^{3+}$) (Gilleo 1958).

Table 1 ***Spin diagrams of crystal field splitting of cation 3d orbitals in the case of tetrahedral (( )T) as well as octahedral ({ }O) symmetries in spinel-type Li-Ni ferrite.***

Cation	Tetrahedral							Octahedral						
		Low Spin	S	High Spin	S		Low Spin	S	High Spin	S				
$Ni^{2+}[Ar]3d^8$	t_{2g}	d_{xy} d_{yz} d_{xz}	3	d_{xy} d_{yz} d_{xz}	3	e_g	d_{x2-y2} d_{z2}	3	d_{x2-y2} d_{z2}	3				
	e_g	d_{x2-y2} d_{z2}		d_{x2-y2} d_{z2}		t_{2g}	d_{xy} d_{yz} d_{xz}		d_{xy} d_{yz} d_{xz}						
$Fe^{2+}[Ar]3d^6$	t_{2g}	d_{xy} d_{yz} d_{xz}	3	d_{xy} d_{yz} d_{xz}	5	e_g	d_{x2-y2} d_{z2}	1	d_{x2-y2} d_{z2}	5				
	e_g	d_{x2-y2} d_{z2}		d_{x2-y2} d_{z2}		t_{2g}	d_{xy} d_{yz} d_{xz}		d_{xy} d_{yz} d_{xz}						
$Fe^{3+}[Ar]3d^5$	t_{2g}	d_{xy} d_{yz} d_{xz}	2	d_{xy} d_{yz} d_{xz}	6	e_g	d_{x2-y2} d_{z2}	2	d_{x2-y2} d_{z2}	6				
	e_g	d_{x2-y2} d_{z2}		d_{x2-y2} d_{z2}		t_{2g}	d_{xy} d_{yz} d_{xz}		d_{xy} d_{yz} d_{xz}						

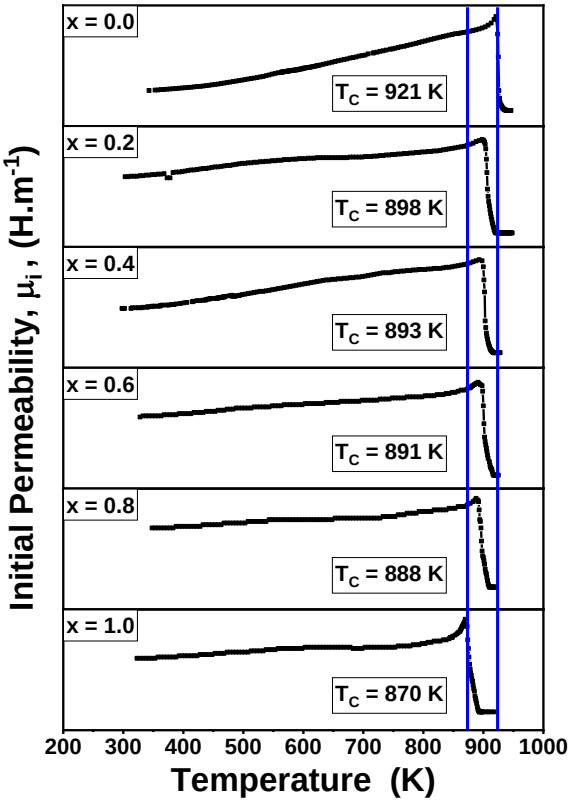

Figure 1 ***Variation of initial permeability, μ_i , with temperature for all samples.***

Real (ε'), imaginary (ε'') and complex (ε^*) dielectric permittivity were calculate according to the relation in ref. (Dawoud et al 2017). They show dispersion with increasing of applied frequency (υ) as given in Figs. 2-4, which are considered as a normal behavior for spinel ferrites (Soibam 2016). As seen in such Figs., dielectric permittivity constants are high when υ is low, but it rapidly declines as υ increases. Space charge polarization (SCP) and Koop's two-layers model help to explain the drop in dielectric permittivity constants (Koop 1951). This model posits that ferrite is made up of grain boundaries that separate well-conducting grains. The electrons jump to the grain boundary and pile up because of its lower conductivity. However, there are two processes $Fe^{3+} + e^- \leftrightarrow Fe^{2+}$ and $Ni^{2+} + h^+ \leftrightarrow Ni^{3+}$. The first one is more dominant (Smit et al 1959). In addition, more existing of Fe^{3+} ions at Oh sublattices, increases jumping process. Consequently, the process of electrons building up at grain boundaries and SCP is accelerated, as a result, dielectric permittivity constants increase. At low υ, a high resistivity grain boundary prevents electrons from jumping and generating SCP, resulting in a high permittivity. As the frequency grows, electrons are unable to follow it, and they reverse direction of motion, limiting the possibility of electrons reaching the grain boundary. Dielectric permittivity constants are subsequently reduced as a result. Polarizability is very modest with larger values of υ, and it becomes independent of υ. Various ferrite systems showed a similar pattern of behavior (Aravind et al 2015).

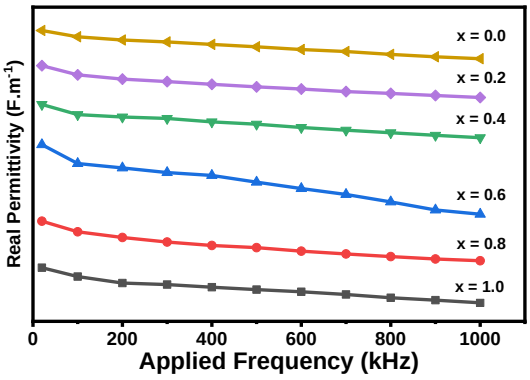

Figure 2 ***Variation of real permittivity versus applied frequency.***

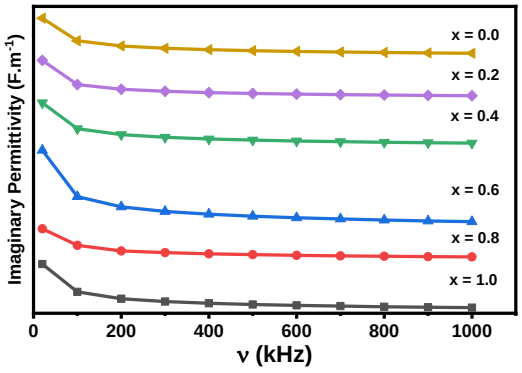

Figure 3 ***Variation of imaginary permittivity versus***

applied frequency.

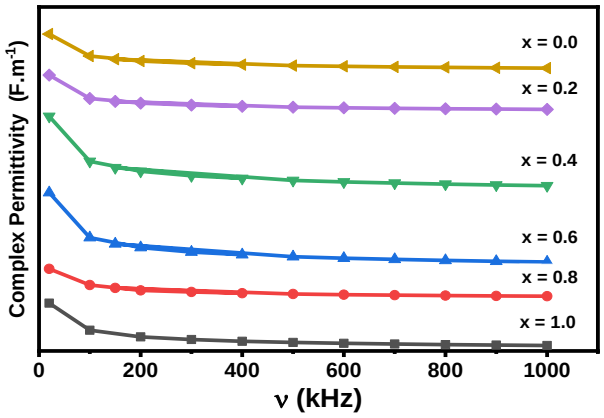

Figure 4 ***Variation of complex permittivity against applied frequency.***

Fig. 5 shows variation of $\tan\delta = \varepsilon''/\varepsilon'$ with υ. Due to decreasing polarization at high frequency, it declines with increasing frequency and stays constant at 1MHz.

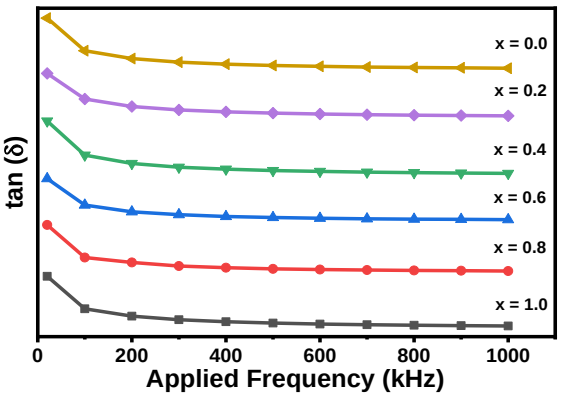

Figure 5 ***Variation of $\tan\delta$ against applied frequency.***

For the prepared samples of spinel ferrite, change of σ_{AC} with υ was investigated (Fig. 6). As given in this Fig. σ_{AC} increases exponentially with increasing of υ, which exhibits normal behavior of ferrites. This is due to the applied force, which aids in the transfer of charge carriers between various conduction states. It's possible that it's caused by electron jumping or exchange, i.e.

$$Fe^{3+} + e^{-} \leftrightarrow Fe^{2+}$$

or

$$Ni^{2+} + h^{+} \leftrightarrow Ni^{3+}$$

This occurs as a result of an electron transfer between adjacent Oh sites (Shaat 2012). The Verwey mechanism can be used to explain the increase in σ_{AC} (Shaat 2012). That is, electron jumping can occur between ions of the same element that exist in a variety of valence states and are dispersed at random across inequivalent sublattices crystal lattice (Dawoud et al 2016). The number of such ions created may vary depending on the sintering circumstances. It is well known that at high firing temperatures, partial reduction of electron jumping, $Fe^{3+} + e^{-} \leftrightarrow Fe^{2+}$, can occur (Shaat 2012). The dispersion is associated with Ni content and is found to decrease as increasing of Ni content. In other ferrite from different investigators, a similar pattern for spinel ferrites was confirmed (Dawoud et al 2010, Shahjahan et al 2014).

Fig. 6 presents the relation between σ_{AC} and υ. A mathematical expression for the relationship between σ_{AC} and υ may be inferred from the fitted curves of Fig. 6 (Dawoud et al 2017)

$$\sigma_{AC}(T,\omega) = b + d\omega^{S(T)} \qquad (2)$$

where $S(T)$ is universal exponential parameter. As a consequence, Eqn. (2) might be used to describe the behaviour of σ_{AC} in a material like this. σ_{AC} can be functioned in (T and ω). Thus; σAC can be described as a function$\sigma_{AC}(T,\omega)$, which is given by (Dawoud et al 2017).

$$\sigma_{AC}(T,\omega) = C(T)\omega^{S(T)} \qquad (3)$$

Applying logarithms for Eqn. (3) yields the following:

$$\ln \sigma_{AC}(T,\omega) = \ln C(T) + S(T) \ln \omega \qquad (4)$$

where $C(T)$ has σAC unit and $S(T)$ with $(0 < S(T) < 1)$. As a result of Eqn. (4), ln σAC is changed linearly with ln ω, as illustrated in Fig. 7. The temperature dependency of these quantities $C(T)$ and $S(T)$ may be explained using the conduction process [1]. $S(T)$using fitting of σ_{AC} curves, as shown in Fig. 6. $S(T)$ was also found using the slope of $\ln \sigma_{AC}$ versus ln υ curves, as illustrated in Fig. 7. The values of $S(T)$ obtained from Fig. 6 and Fig. 7 are shown in Table 2. The acquired results are consistent with other workers' reported values (Azadmanjiri 2008, Alwash et al 2016, Pervaiza et al 2012).

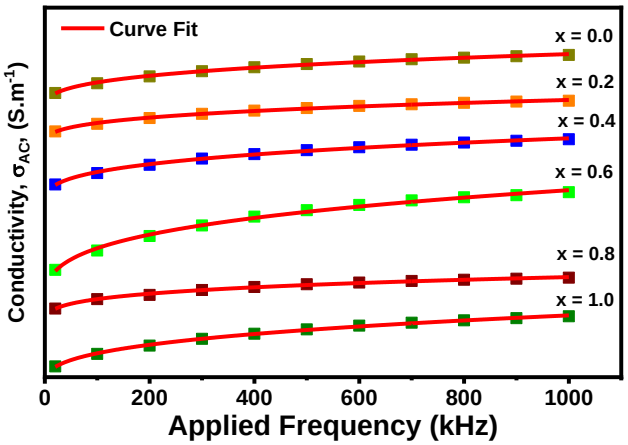

Figure 6 ***Variation of σ_{AC} against applied frequency with red curve fit.***

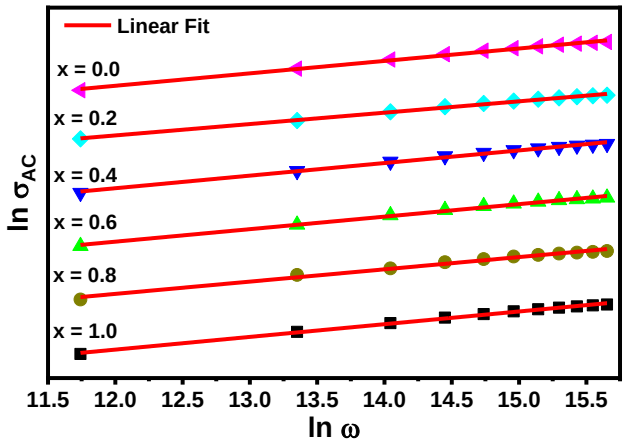

Figure 7 ***Fitted $\ln \sigma_{AC}$ against $\ln \omega$ with red linear fit.***

Table 2 ***The values of S(T) obtained from Fig. 6 and Fig. 7.***

x	S(T) Fig. 6	S(T) Fig. 7
0.0	0.33508 ± 0.02466	0.44612 ± 0.00776
0.2	0.2361 ± 0.03501	0.43093 ± 0.01554
0,4	0.28804 ± 0.03973	0.43911 ± 0.01045
0,6	0.29901 ± 0.02879	0.44247 ± 0.00991
0,8	0.29645 ± 0.003371	0.39893 ± 0.00706
1.0	0.29376 ± 0.03023	0.43599 ± 0.00973

4. Conclusion

The substitution of Ni^{2+} ions have a significant impact on the electric and dielectric properties of Li spinel ferrite. We came to the following conclusions as a result of this research:

- The Curie temperature points T_C decreasing as the number of Ni^{2+} ions rise.
- For all samples, dielectric permittivity constants decrease as applied frequency increases.
- Due to decreasing polarization at high applied frequency, $\tan \delta$ decreases with rising of υ and becomes constant up to = 1MHz
- As applied frequency increasing σ_{AC} increases for all samples.

DATA AVAILABILITY STATEMENT:

The data that support the findings of this study are available from the corresponding author upon reasonable request.

CONFLICT OF INTEREST:

The authors declare that they have no conflict of Interest that could have appeared to influence the work reported in this manuscript.

FUNDING:

The authors declare that there is no funding for this manuscript.

REFERENCES.

Alwash N. H., Mohamad H. K., Almaamori M. H., (2016) Effect of M^{2+} substitution on properties of the system $Ni_xZn_{1-x-y}MyFe_2O_4$, *International Letters of Chemistry, Physics and Astronomy*, 63, 42-48.

Aravind, G., Raghasudha, M. and Ravinder, D. (2015) Electrical transport properties of nano crystalline Li–Ni ferrites, *Journal of Materiomics*, 1(4), 348-356.

Azadmanjiri, J., (2008) Structural and electromagnetic properties of Ni–Zn ferrites prepared by sol–gel combustion method, *Materials Chemistry and Physics*, 109(1), 109–112.

Dawoud, H. A., AH Elhillo, E. A., & Shaat, S. K. K. (2018). Investigation of structural parameters and magnetic properties of mixed Li-Ni spinel ferrites, *International Journal of Chemical and Physical Sciences*, 7(3), 92-103.

Dawoud, H. A., S. K. K Shaat & Yassin, S. S. (2010). AC conductivity and dielectric properties of Cu–Zn ferrites. *Journal of Al Azhar University-Gaza (Natural Sciences)*, 12, 65-74.

Dawoud, H., Abu Mosa, Z., & Shaat, S. (2017). Synthesis and AC properties of mixed Li-Zn ferrites. *International Journal of Current Research*, *9*(10), 59176-59179.

Dawoud, H., Abu Mosa, Z., & Shaat, S. (2018). Structural parameters and magnetic susceptibility of mixed Li-Zn spinel ferrites. *American Journal of Chemistry and Materials Science*, *5*(1), 10-19.

Dawoud, H., A-Ouda, L. & Shaat, S. K. K. (2016). Investigation of the effect of Zn ions concentration on DC conductivity and Curie temperature of Ni-spinel ferrite. *American Journal of Materials Science and Application*, 4(2), 11-17.

Dawoud, H., A-Ouda, L. & Shaat, S. K. K. (2016). Synthetize and magnetic properties of Ni substituted polycrystalline Zn-spinel ferrites. *International Journal for Research in Applied Science and Engineering Technology*, *4*(XII), 111-118.

Dawoud, H., A-Ouda, L. and Shaat, S. K. K. (2017). AC and dielectric properties of polycrystalline Zn–Ni spinel ferrites prepared by double sintering technique. *IUG Journal of Natural Studies*, *25*(2), 274-281.

G. Aravind, D. Ravinder, and V. Nathanial, (2014) Structural and Electrical Properties of Li–Ni Nanoferrites Synthesised by Citrate Gel Autocombustion Method, *Physics Research International*, 2014, 1-11.

Gilleo, M. A., (1958) Superexchange Interaction Energy for Fe3+-O2−-Fe3+ Linkages, *Physical Review*, 109(3), 777–781. https://doi.org/10.1103/PhysRev.109.777

Khot Sujata, S., Shinde, N. S., Kale, B. B, Basavaiah, N., Watawe, S. C., Vaidya, M. M., (2014) Microstructure

and Infrared Absorption Spectroscopic Study of Zn Substituted Li-Cu Ferrites, *International Journal of Chemical and Physical Sciences*, 3(Special Issue 3, NCRTSM), 107-116.

Koop, C. G., (1951) On the Dispersion of Resistivity and Dielectric Constant of Some Semiconductors at Audiofrequencies *Physical Review*, 83(1), 121-124. https://doi.org/10.1103/PhysRev.83.121

Mazen S. A. and Dawoud H. A., (1999), Structure and magnetic properties of Li-Cu ferrite, Phys. Stat. Sol. (a), 172(2), 275-289.

Pervaiza E. and Gula I. H., (2012) Structural, Electrical and Magnetic Studies of Gd^{3+} doped Cobalt Ferrite Nanoparticles, *NPRESSCO*, 2(4), 377- 387.

Shaat, S. K. K., (2012) Advanced Ferrite Technology, LAMBART Academic Publishing.

Shahjahan Md., Ahmed N. A., Rahman S. N., Islam S., Khatun N., (2014) Structural and Electrical Characterization of Ni-Zn Ferrites, *IJETCAS*, 13(104), 20-25.

Smit, J. and Wijn, H. P. J., (1959) Ferrites, New York: John Wiley.

Soibam I., (2016) A Study of Microwave Sintered Ni Substituted Lithium Zinc Ferrite Synthesized by Citrate Precursor Method*, International Journal of Materials Science and Engineering*, 4(1), 2016, 54-59.